A Consumer-Centric Approach to Energy Management System Modeling

1st Mirela Dobra
Automation dept.
TU of Cluj-Napoca
Cluj-Napoca, Romania
mirela.trusca@aut.utcluj.ro

2nd Ionut Dragos Roman
Automation dept.
TU of Cluj-Napoca
Cluj-Napoca, Romania
Ionut.Roman@campus.utcluj.ro

3rd Mircea Raceanu
Institute for Cryogenics and Isotopic Technologies
Rm Valcea, Romania
mircea.raceanu@icsi.ro

***Abstract*—This work supports the development of an smart grid energy management framework based on an experimentally validated photovoltaic (PV) system consisting of real PV panels connected to a grid-forming inverter. The study begins with experimental measurements obtained from the PV system under realistic irradiance and load conditions, enabling the evaluation of system efficiency and transient response. Building on this validated foundation, an operational scheduling strategy is developed to improve supply continuity and mitigate the effects of intermittent solar power production. The scheduling strategy is experimentally bench-marked to evaluate power-sharing capability, voltage regulation, and load-following performance when supplying low-power household appliances. The results clearly demonstrate the technical feasibility and operational effectiveness of implementing a simple scheduling-based energy management strategy, capable of optimizing power allocation according to generation availability and load demand, thereby improving system reliability, operational flexibility, and continuity of supply in small-scale residential applications.**

***Index Terms*—Hybrid Energy Storage System (HESS), PV invertor, Gel Battery, cumulative energy, residential appliances**

I. Introduction

A real hardware benchmark plays a fundamental role in the development and validation of Energy Management System (EMS) control algorithms, as it enables the assessment of practical operating conditions that are often overlooked or simplified in simulation environments. While simulation models provide a valuable framework for preliminary design and analysis, they typically rely on idealized assumptions that do not fully capture the behavior of physical components. In real implementations, power electronic converters, sensors, communication networks, and energy storage devices are affected by non-ideal characteristics such as switching and communication delays, signal quantization, hysteresis effects, thermal variations, parameter uncertainties, component aging, and measurement noise. These factors can lead to significant discrepancies between the modeled and actual system behavior, commonly referred to as model–plant mismatch. Consequently, an EMS strategy that demonstrates satisfactory performance under simulation conditions may experience degraded efficiency, slower dynamic response, undesired oscillations, poor power-sharing performance, or even instability when deployed on real hardware [5]. Experimental benchmarking therefore provides a critical validation stage, allowing control algorithms to be evaluated under realistic operating conditions and ensuring their robustness, reliability, and practical applicability before large-scale deployment.

This work was supported by a grant co-financed by the European Regional Development Fund, within the Smart Growth, Digitization and Financial Instruments Program 2021-2027, as part of project Romanian Hub for Hydrogen and new energy technologies-Ro-HydroHub, contract no G 2025-113330 din 30.09.2025 to G 2024-81692/390006 from 13.11.2024, SMIS code: 351358

II. Energy Management System architecture

The adopted architectural description for the Hybrid Energy Storage System (HESS) is similar to existing work like [5]. It integrates multiple distributed energy resources (DERs), power conversion stages, protection elements, and a supervisory Energy Management System (EMS). The architecture is structured around a common DC bus that interfaces renewable sources, electrochemical storage, dispatchable generation, and the utility grid.

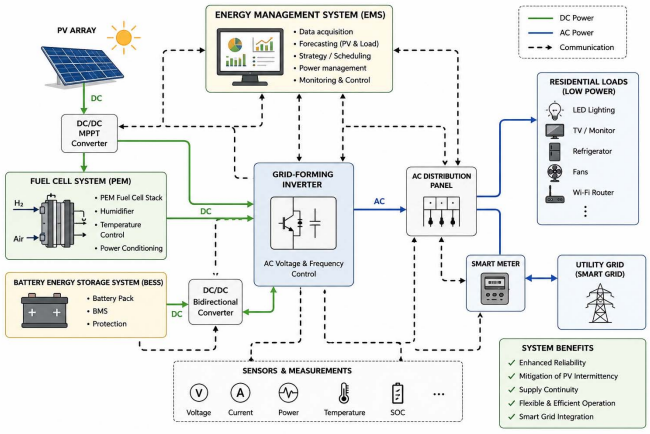

Fig. 1. HESS Architecture

This DC-coupled HESS topology in Fig. 1 is inherently scalable [4] because additional generation sources, storage units, or converter modules can be paralleled onto the common DC bus with minimal architectural modification. Its modular power electronics and centralized EMS enable expansion from small kW-scale microgrids to multi-MW hybrid plants while maintaining coordinated control and protection logic [2].

III. Test Bench Setup

The test bench setup in features a hybrid solar power and monitoring system composed of a hybrid off-grid inverter and a deep-cycle battery bank. The system is integrated with a laptop for real-time data analysis and performance tracking.

The main unit is a Voltronic hybrid inverter having 3kVA to 5kVA. These devices combine the functions of a pure sine wave inverter, an MPPT solar charge controller, and a battery charger into a single integration. This setup handles power range of maximum 5kVA with a power factor of 1. The system is powered by six Poly crown 470W mono crystalline solar panels. This panel feature 120 half-cut cells, a design that improves efficiency and performance in shaded conditions compared to standard full-cell panels. Energy storage consists of four Ultracell UCG200-12 VRLA Gel batteries. Each battery provides 12V and 200Ah of capacity [6], [7]. They are wired in series to create a 48V DC bank, matching the input requirements of the 5kVA inverter. A laptop is integrated into the setup, connected via a data cable to the inverter's communication port 2. It runs specialized software [8] to monitor critical metrics such as PV input wattage, battery state of charge, and output load levels [3].

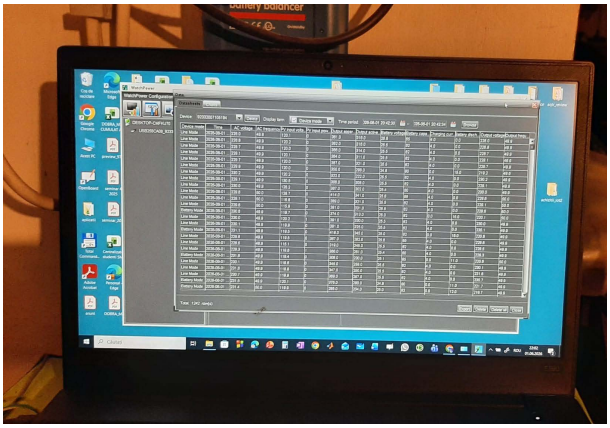

Fig. 2. Laptop runing watchport software

A. Data Processing

The experimental data collected from the inverter monitoring system were imported into MATLAB using the Import Tool and stored in a table format (Fig. 3) for subsequent analysis. During the import process, the first row of the spreadsheet was defined as the variable names row, allowing MATLAB to automatically assign column headers corresponding to the measured parameters, such as operating mode, AC voltage, AC frequency, PV input voltage, PV input power, output apparent power, output active power, battery voltage, battery capacity, charging current, discharge current, output voltage, and output frequency.

To ensure data consistency, MATLAB was configured to identify and handle non-importable or incompatible cells. Any entries that could not be directly interpreted according to the selected data type were automatically replaced with NaN (Not-a-Number) values or converted to the closest compatible format. This preprocessing step prevents data corruption and facilitates subsequent numerical computations. For example, cells containing mixed text and numerical values were converted into a uniform representation to maintain the integrity of the dataset. Once imported, the table structure enabled efficient

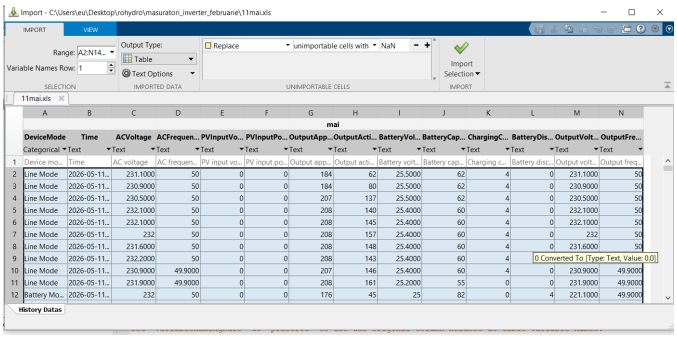

Fig. 3. Data stored in a table format

access to individual variables using their corresponding column names. The time stamps were extracted and synchronized with the electrical measurements to preserve the chronological order of the recorded events. Numerical variables were then converted into appropriate MATLAB data types, allowing statistical analysis, signal processing, and visualization functions to be applied directly.

Additional preprocessing operations included the detection of missing values, removal of invalid records, verification of measurement ranges, and filtering of abnormal or inconsistent samples. The processed data were subsequently used to evaluate the operating behavior of the photovoltaic-inverter system under different load conditions, including the assessment of power flow, voltage regulation, frequency stability, battery state evolution, and energy conversion performance.

This systematic preprocessing procedure ensures that the imported measurements accurately reflect the behavior of the real hardware system and provides a reliable database for the development, validation, and benchmarking of energy management and control algorithms in MATLAB.

IV. Energy Consumption Patterns

Based on real measurements in Fig. 4, the consumer's habits are characterized by significant, intermittent power surges rather than a steady baseline load. The spikes, present in the "Output Apparent Power" indicate the use of high-draw appliances at specific times. The morning peak (7:30) as a sharp increase in demand up to 2000W, corresponds to a washing machine; late morning peak (10:00 - 10:30) indicates another surge exceeding 2000W which corresponds to a dishwasher. Mid-day activity (13:30) under an isolated spike shape matches the brief use of a high-power device (electric stove). The evening peak (17:30 - 18:00) resembling like a multiple rapid spikes reaching 2000W corresponds again to a high-power device (air fryer) followed by washing machine spike pattern (after 18:00).

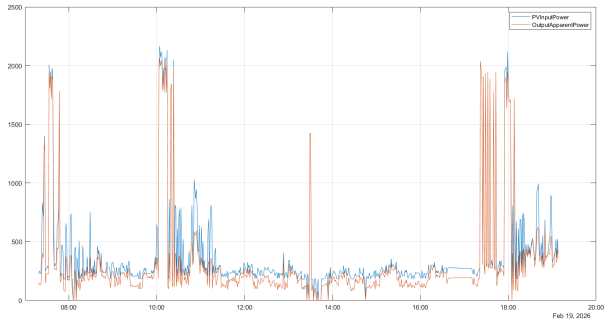

Fig. 4. Active Power over daylight

A. Solar energy pattern

The performance of photovoltaic (PV) system can be evaluated for one day with he measurements in Fig. 5.

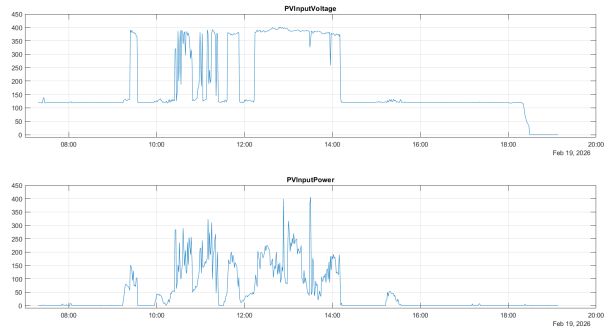

Fig. 5. Solar energy production

The PV Input Voltage (first subplot) analysis shows that for a significant portion of the day, approximately between 07:00 and 09:30 and again from 14:15 to 18:30, the voltage remains constant at around 120 V. This level typically represents the open-circuit voltage or a minimum operating threshold when the inverter is powered on but not drawing substantial energy from the panels. During peak solar irradiance, particularly between 12:30 and 14:00, the voltage stabilizes near 400 V, indicating that the system is operating under load and tracking its Maximum Power Point (MPP). Noticeable fluctuations occur between 10:30 and 12:00, where the voltage exhibits significant variability. This behavior is consistent with intermittent cloud cover or rapid changes in shading or load conditions. After 18:00, the voltage drops to 0 V, which corresponds with sunset and the cessation of solar generation.

The PV Input Power (second subplot) analysis reveals that the system achieves its maximum power output of approximately 400 W between 12:30 and 14:00. However, the power curve is considerably more erratic than the voltage profile. Even though the voltage remains elevated and relatively stable during peak hours, the power output fluctuates significantly, a pattern that is typical when variable cloud cover intermittently reduces irradiance on the panels. A particularly notable feature appears around 14:15, when the power output drops to zero and remains flat despite the voltage holding steady at the 120 V baseline. This indicates that although the panels were electrically active, no usable current was being drawn. Such behavior is the result from heavy shading, but may occurs as a protective system shutdown, inverter-related constraints, or a fully charged battery in an off-grid configuration.

Overall, the system appears to respond appropriately to available light conditions, suggesting that its fundamental operation is correct. However, the pronounced variability and the early cessation of power production strongly suggest that the day was characterized by significant cloud cover. The most critical observation is the discrepancy between sustained baseline voltage and zero power output after 14:15, which indicates that the array remained energized but was not delivering energy to the load or storage system.

B. Solar Utilization and efficiency

Measurements plotted in Fig. 6 present the performance of the photovoltaic (PV) system with battery storage throughout one entire daylight evaluating the behavior based on the three monitored parameters.

The Output Active Power section shows noticeable consumption peaks exceeding 2000 W between 10:00 and 10:30 and again between 17:30 and 18:00. These peaks indicate periods when high-power household appliances were in use. During the rest of the day, the output power remains relatively low and stable, around 200–300 W, which reflects the base load from continuously operating devices such as the refrigerator, router, and other common equipment.

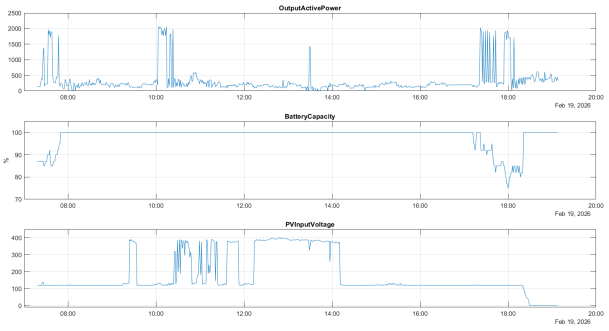

Fig. 6. Solar and habits correlation

The *Battery Capacity* data in the second subplot indicates that the battery started the day at approximately 85% and reached 100% around 08:00, benefiting from early solar production or a prioritized charging setting. The battery remained at full capacity from 08:00 until 17:30, demonstrating that solar generation was sufficient to cover household consumption while keeping the battery fully charged. After 17:30, as solar production declined and consumption increased, the battery began to discharge rapidly, reaching a minimum level of approximately 77%.

The PV Input Voltage in the third subplot, shows that the solar panels began generating significant voltage after 09:30. Voltage fluctuations between 120 V and 400 V can be observed, most likely due to passing clouds or the inverter's Maximum Power Point Tracking (MPPT) algorithm adjusting operating conditions. Between 12:30 and 14:00, the voltage remained highly stable at approximately 380 V, indicating steady and optimal solar production. After 18:30, solar generation ceased completely, as shown by the voltage dropping to 0 V at sunset.

In conclusion, the system operated correctly throughout the day. Solar production was sufficient to maintain the battery at full capacity during daylight hours, and the battery effectively supported the high evening loads around 18:00 when the panels were no longer producing energy.

C. Power balance evaluation

PV Input Power (blue) and *Output Apparent Power* (red) comparison in Fig. 7 reveals a significant imbalance throughout the day, indicating that the system's generated solar energy often does not meet the immediate load demand. For

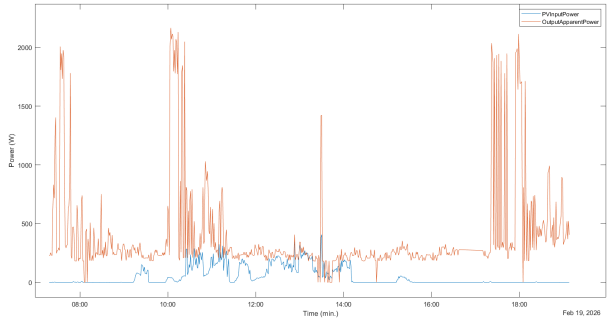

Fig. 7. Power balance

Output Apparent Power, the large spikes reaching 2000W at approximately 08:00, 10:00, and 18:00 indicate transient heavy loads. During these times, PV input is nearly zero or very low, meaning the entire load is being carried by the grid. Making the mid-day correlation, between 11:00 and 14:00, the PV Input Power increases and partially matches the base load (250W). In some brief moments (e.g., around 13:30), PV input actually exceeds the apparent power. In a hybrid system, this surplus would be used to recharge batteries or power an electrolyzer for hydrogen production.

Hybrid Sizing with Buffer Storage

A more technically and economically balanced solution consists of combining a moderately sized fuel cell with a small battery buffer. The sustained deficit over most of the operating period appears to lie between $0.3\,\mathrm{kW}$ and $0.4\,\mathrm{kW}$. Therefore, selecting a fuel cell rated between $0.8\,\mathrm{kW}$ and $1.0\,\mathrm{kW}$ allows steady-state operation near its optimal efficiency point, while short transient peaks are absorbed by the battery.



Fig. 8. Power balance, shortened time window

The required battery energy capacity corresponds to the integral of the residual deficit above the fuel cell rating,

$$E_{\mathrm{bat}} = \int \left(P_{\mathrm{load}}(t) - P_{\mathrm{supplied}}(t) - P_{\mathrm{FC,rated}}\right)^{+} dt, \quad (1)$$

where $(\cdot)^{+}$ denotes the positive part. Based on the short-duration spikes visible in the profile, an estimated storage capacity of approximately $0.3\,\mathrm{kW\,h}$ to $0.5\,\mathrm{kW\,h}$ would be sufficient (a 9.6kWh is already available together with the PV panels).

V. Cumulative Energy Based Approach

Having a control-systems perspective, the cumulative formulation is generally superior. It preserves causality, enables real-time computation, integrates naturally into state-space models, and supports feedback design and observer construction. The area-under-the-curve approach is appropriate when only a retrospective scalar metric is required, but it lacks structural compatibility with dynamic system analysis. Therefore, when modeling, simulation, or control integration is required, representing energy in cumulative manner [1], [7] is the more robust and theoretically consistent approach.

The use of cumulative energy curves over short time windows in Fig. 9 follows similar methodology based on *ramp rate* calculation, where segmented energy balance highlights transient mismatches between PV input and load demand.

A practical solution, easy to implement, stands in designing supervisory energy-management layer that monitors cumulative energy imbalance over short windows and commands PWM duty-cycle corrections in the converter stage having the derived shaped in Fig 10. The PWM operates on a fast time scale, while the cumulative energy window provides a slow-time-scale indicator of net imbalance. This hierarchical approach links short-window cumulative crossover events to actionable switching control.

VI. Weather Impact

Power production over a larger than one day period in Fig. 11 displays a highly intermittent profile characterized by significant fluctuations throughout the day. The data shows that peak generation occurs primarily between 11:00 and 15:00, with maximum power outputs varying significantly, ranging

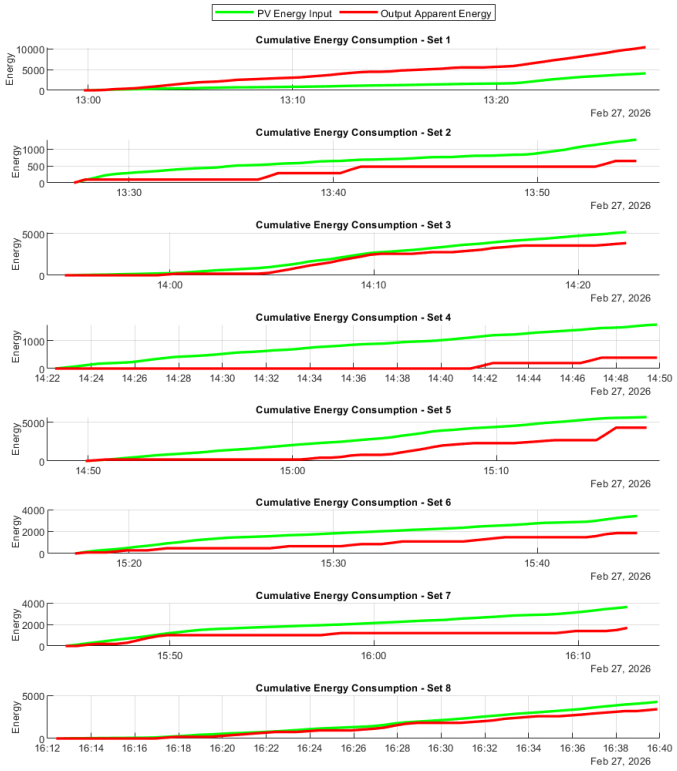

Fig. 9. Power balance, shortened time window

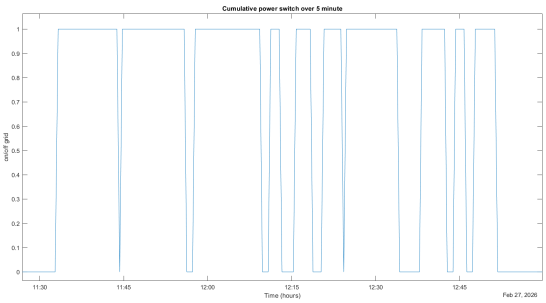

Fig. 10. PWM duty-cycle corrections based on power balance

from under 500W to nearly 2000W across different days. Weather records for Cluj during this period indicate average temperatures around 3°C and frequent cloud cover (roughly 54% overcast), which explains the inconsistent power curves and sharp production drops.

Notably, February 27 and 28 show the most substantial spikes in production, aligning with historical data that identifies February 28 as one of the clearest days of the month. Overall, this specific week highlights the impact of winter seasonality and variable cloudiness on solar reliability.

Even during the ”weakest production period” illustrated with measurement in Tabel I, the PV system provides a critical buffer. The PV system produced a total average of 583290 W, covering roughly 15.4% of the total energy demand. Without these panels, the grid dependency would have reached 100%,

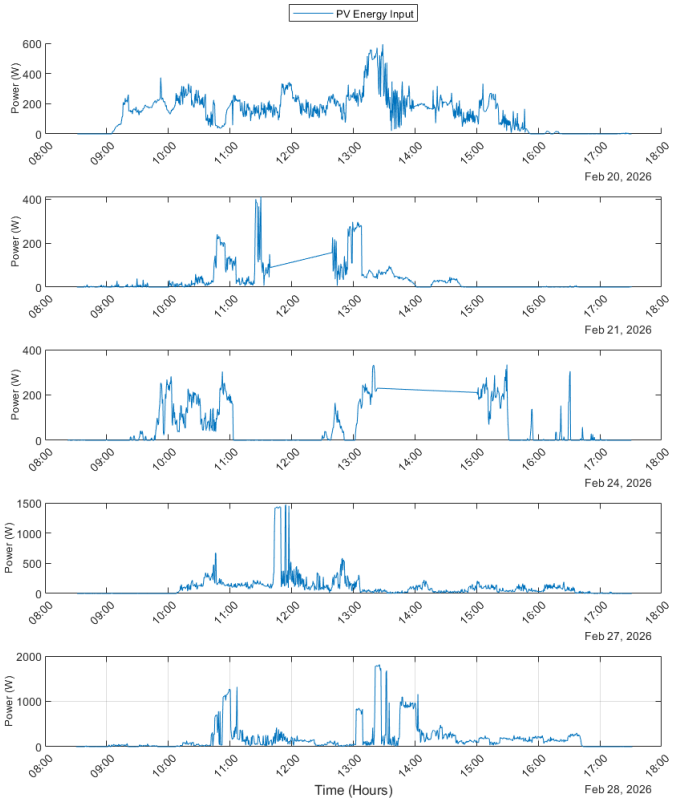

Fig. 11. Winter seasonality impact on PV power production

significantly increasing operational risks during peak demand. PV inclusion remains a sound investment for peak shaving. However, the high ”PV deficit” (averaging 80%) confirms that during winter or low-exposure months, PV cannot be a standalone solution and requires robust hybridization.

Date	PV supplied (%)	PV deficit (%)	PV excess (%)	Grid consume (kW)	PV produced (kW)	kWh price (RON)	kWh price ($)
19 Febr.	12.2	88.1	0.3	270322	34063	7.20	1.413
20 Febr.	19.8	80.3	0.1	773540	152782	20.62	4.04
21 Febr.	8.8	91.8	0.6	353628	31215	9.43	1.84
22 Febr.	32.2	67.8	0	488692	15732	13.03	2.55
24 Febr.	13.2	87	0.1	355321	46809	9.47	1.85
27 Febr.	27.1	77.5	4.7	403887	109552	10.77	2.12
28 Febr.	34.4	67.4	1.9	560857	193137	14.95	2.93

TABLE I
PV PRODUCTION AND GRID CONSUMPTION DATA FOR FEBRUARY 2026, 1.6 RON /KWH APROXX. 0.3 EUR /KWH

VII. FULL COVERAGE

Short evaluation regarding PV coverage plots in Fig. 12 indicate that the photovoltaic (PV) system provides its highest contribution between approximately 08:00 and 20:00, with peak generation occurring around 13:00–14:00, where the PV input power reaches values above 2 kW. During this period, the PV production closely follows and partially covers the load demand, reducing the dependence on the battery and external energy sources. This improved PV coverage is also reflected in the Battery Capacity profile, which increases from about 60% in the morning to nearly 100% around midday, demonstrating

that excess solar energy is available for battery charging. The extended interval during which the battery remains fully charged further confirms that PV generation exceeds the instantaneous load demand for a significant portion of the day. Overall, the results demonstrate effective solar energy utilization, enhanced load coverage during daylight hours, and improved energy autonomy of the system.

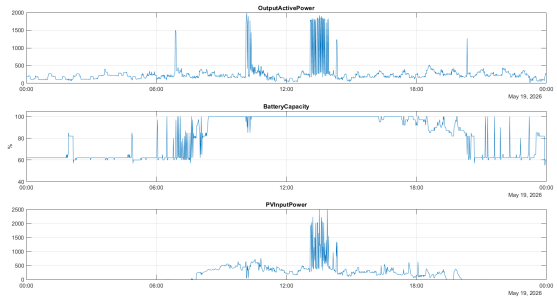

Fig. 12. Power production at full capabilities

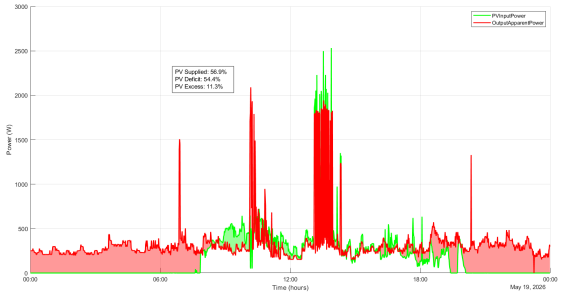

Fig. 13. Power production over daylight fully covered

VIII. Scheduling-Based Energy Management Strategy

Four main directions in making a Scheduling-Based Energy Management Strategy can be overrefined.

Load scheduling based on solar availability aims to align flexible household loads, such as washing machines, water heaters, and electric vehicle charging, with periods of high photovoltaic (PV) generation. By shifting energy-intensive activities toward peak solar production hours, direct utilization of renewable energy is maximized while dependence on battery storage and grid imports is reduced.

Battery-aware energy management must prioritize battery charging during periods of surplus PV production and reserve stored energy for evening and nighttime consumption, ensuring supply continuity while minimizing deep discharge cycles and extending battery lifetime.

Dynamic power balance optimization should assure continuously match energy demand with available PV generation and battery state of charge, limiting non-essential loads during low-generation periods and maintaining a balanced and efficient operation of the hybrid energy system.

Consumer guidance and demand response can provide users with real-time recommendations on the most suitable periods for operating high-energy appliances, along with notifications regarding expected solar production, battery status, and potential energy savings to encourage more efficient consumption habits.

IX. Conclusion

The analysis demonstrates that significant and continuous improvements can be achieved through the implementation of an advanced Energy Management System (EMS) that not only optimizes the coordination between photovoltaic generation, battery storage, and load demand, but also actively interacts with the end user. By incorporating consumer behavior into the decision-making process, the EMS can increase renewable energy utilization, reduce energy costs, and enhance overall system efficiency. Future developments should therefore focus on strengthening the interaction between the EMS and the final consumer through intelligent decision-support mechanisms and adaptive scheduling strategies.

The EMS can provide personalized consumption recommendations by analyzing user habits, solar generation forecasts, and available energy resources, thereby helping consumers schedule appliance operation during the most favorable periods to maximize self-consumption and reduce energy costs.

A higher level of interaction between the EMS and the consumer can be achieved through real-time notifications and operational recommendations, enabling users to adapt their consumption patterns according to current photovoltaic production, battery status, and energy demand conditions.

The integration of predictive energy planning capabilities would allow the EMS to combine weather forecasts, load predictions, and battery state information to generate optimized operating schedules while providing feedback on energy savings and renewable energy utilization.

References

[1] Chrysanthos Charalambous, Alexis Polycarpou, Venizelos Efthymiou, and George E Georghiou. Enhancing energy efficiency and sustainability with hybrid ac/dc microgrids for energy transition. In *2024 3rd International Conference on Energy Transition in the Mediterranean Area (SyNERGY MED)*, pages 1–5. IEEE, 2024.

[2] Robert W Erickson and Dragan Maksimovic. *Fundamentals of power electronics*. Springer Science & Business Media, 2007.

[3] Lisa Gitelman. *Raw data is an oxymoron*. MIT press, 2013.

[4] Dan Hulea, Mihăiță Gireadă, Octavian Cornea, and Nicolae Muntean. An improved bidirectional hybrid switched capacitor converter. In *IECON 2022–48th Annual Conference of the IEEE Industrial Electronics Society*, pages 1–6. IEEE, 2022.

[5] Desmond Eseoghene Ighravwe and Daniel Mashao. Analysis of energy storage technologies using consumers expectations. In *2021 International Conference on Electrical, Computer and Energy Technologies (ICECET)*, pages 1–5. IEEE, 2021.

[6] International Energy Agency. Global hydrogen review 2023, 2023.

[7] Inoussa Legrene, Tony Wong, and Louis-A Dessaint. Practical cost effectiveness analysis for solar energy systems: case study of stand-alone retail building. In *2024 IEEE 18th International Conference on Compatibility, Power Electronics and Power Engineering (CPE-POWERENG)*, pages 1–5. IEEE, 2024.

[8] Voltronic Power Technology Corp. *WatchPower User Manual*. Voltronic Power Technology Corp., Taiwan, 2023. Monitoring software for Axpert and compatible hybrid inverters.